



Study of the post-combustion CO₂ capture process by absorption-regeneration using amine solvents applied to cement plant flue gases with high CO₂ contents



Sinda Laribi, Lionel Dubois, Guy De Weireld, Diane Thomas*

Chemical & Biochemical Process Engineering and Thermodynamics Units, Faculty of Engineering, University of Mons, 20 Place du Parc, 7000 Mons, Belgium

ARTICLE INFO

Keywords:

Post-combustion CO₂ capture
Absorption-regeneration process
Amine(s)-based solvents
Aspen Hysys™ simulation
Partial oxyfuel cement plant flue gases
High CO₂ contents

ABSTRACT

The present study is focusing on the investigation, for the cement industry, of the post-combustion CO₂ capture process using amine(s)-based solvents. The novel aspect of the work is the flue gas considered, namely the high CO₂ contents (between 20 and 60 vol.%), representative of flue gases coming from oxygen-enriched air combustion process (also called partial oxy-fuel combustion). Using the results of preliminary solvents screening tests at laboratory scale, absorption-regeneration micro-pilot experiments were carried out for the best solvents in order to characterize their respective absorption and regeneration performances. The use of the activated solution of DEA (diethanolamine) 30 wt.% with PZ (piperazine) 5 wt.% led to particularly high absorption performances in all CO₂ concentration range. Besides the experimental measurements, Aspen Hysys™ simulations of the micro-pilot tests were performed for three solvents (monoethanolamine (MEA) as the reference case, then PZ and DEA + PZ) to validate the models implemented. Finally, the validated models were used to perform industrial scale simulations. These simulations confirmed that both the regeneration energy, the equivalent work and the operating costs are reduced when the absorption-regeneration process is implemented to flue gases with high CO₂ contents.

1. Introduction

To reduce CO₂ emissions from fossil fuels or industrial processes utilization, post-combustion capture by absorption-regeneration or oxy-fuel combustion capture are promising technologies. However, solvent regeneration costs reaching from 3 to 4 GJ/t_{CO₂} in the case of MEA 30 wt.% solvent (van der Spek, 2017) and the large amount of high-purity O₂ production from the Air Separation Unit (ASU) make respectively the post-combustion capture and the oxy-fuel combustion capture energy intensive processes (Gerbelová et al., 2017).

In order to reduce the CO₂ emissions from industrial plants, a more innovative, and hybrid, capture technique was considered in the present work, namely the “partial oxy-fuel combustion CO₂ capture”. The approach of considering hybrid technologies is also presented in the works of (Wang et al., 2017) which gives an overview of different post-combustion CO₂ capture processes applied to coal-fired power plants, including a combination of an absorption-regeneration unit and membranes.

The technology studied in the present paper combines an O₂-enriched air combustion involving a more CO₂-concentrated flue gas

(between 20 and 60 vol.%) compared to the one issued from a conventional combustion and allowing the application of a CO₂ post-combustion capture using amine solvents. This technology presents a double interest. Firstly, in comparison with a full oxy-fuel combustion plant, the amount of oxygen needed to perform the combustion is reduced, which consequently reduces the size of the ASU used for the pure oxygen production (Smart and Riley, 2012). Secondly, and as for example shown by (Doukelis et al., 2009), such technique is expected to decrease the solvent regeneration energy by tons of CO₂ captured in the post-combustion CO₂ capture plant in comparison to conventional conditions. These conclusions have been confirmed by several authors, as highlighted in the literature review presented in Table 1.

Among the key conclusions arising from the literature review presented in Table 1, it can be noted that the post-combustion CO₂ capture applied to O₂-enriched air combustion has not been implemented in the cement industry yet. For example, the ECO-SCRUB project (Adeosun et al., 2013; Smart and Riley, 2012; Doukelis et al., 2009) studied this option for reducing the energy consumption of the CO₂ capture applied to coal-fired power plant flue gases. In the framework of this project, a new pilot-scale oxy-fuel combustion test facility, combined with a

* Corresponding author.

E-mail address: diane.thomas@umons.ac.be (D. Thomas).

Nomenclature	
A	absorption ratio (%)
$\alpha_{\text{CO}_2, \text{rich/lean}}$	CO ₂ loading of the rich/lean solution (mol CO ₂ /mol amine)
ABS	relative to the absorption column
AHPD	2-amino-2-hydroxymethyl-1,3 propanediol
AMP	2-amino-2-methyl-1-propanol
C _{amine}	amine concentration of the solvent (mol/l or wt.%)
C _{CO₂}	amount of CO ₂ absorbed in the solvent (mol CO ₂ /l)
Consumption-U	process consumption of the utility "U" (MW or t/h)
Cost-U	utility cost of "U" (€/MWh)
$\Delta\alpha$	CO ₂ cyclic capacity (mol CO ₂ /mol amine)
DEA	diethanolamine
E _{regen}	specific solvent regeneration energy (GJ/t _{CO₂})
η_{turbine}	power plant turbine efficiency (%)
G	gas flow rate (m ³ /h)
G _{CO₂,abs}	amount of captured CO ₂ (t _{CO₂} /h)
,in	amount of CO ₂ the absorber inlet (/h)
,out	amount of CO ₂ the absorber outlet (/h)
Hum	humidity level of the gas phase (molar fraction)
H _p	column packing height (m)
IC	inorganic carbon
L	liquid flow rate (m ³ /h)
MDEA	methyldiethanolamine
MEA	monoethanolamine
OPEX	total operational expenditure (€/t _{captured CO₂})
OPEX-U	OPEX relative to the utility "U" (€/t)
P _{boiler}	boiler heating power of the micro-pilot unit (kW)
PZ	piperazine
REGEN	relative to the regeneration column
T _{ABS,in}	liquid temperature at the inlet of the absorber (°C)
T _{boiler}	liquid temperature at the bottom of the regeneration column (°C)
T _C	steam condensation temperature in the power plant turbine (°C)
TC	total carbon
TETRA	triethylenetetramine
T _H	steam temperature in the reboiler (°C)
T _{preh,out}	liquid temperature at the outlet of the preheater (°C)
W _{compressors}	compressors electrical energy consumption (GJ/t _{CO₂})
W _{equ}	total equivalent thermodynamic work (GJ/t _{CO₂})
W _{pumps}	pumps electrical energy consumption (GJ/t _{CO₂})
Y _{CO₂,in}	CO ₂ content of the gas phase at the inlet of the absorber (vol.%)
,out	CO ₂ content of the gas phase at the outlet of the absorber (vol.%)
,regen	CO ₂ content of the gas phase at the outlet of the stripper (vol.%)

Table 1

Literature review regarding the partial-oxyfuel CO₂ capture process and high CO₂-contents conditions.

References	Some of the key conclusions
(Lawal et al., 2010) (Lawal et al., 2011) (Kemper et al., 2011)	Dynamic modeling and effect (e.g. decrease of reboiler duty) of increasing CO ₂ partial pressure in flue gas on the CO ₂ capture plant using amine-based chemical absorption (MEA 30 wt.%) was investigated. The study shows that a significant improvement of the absorption process occurred for different solvents tested when pure CO ₂ was used, suggesting an enhancement of the CO ₂ absorption process when higher CO ₂ concentrations are present in the flue gas.
(Favre et al., 2009) (Belaissaoui et al., 2012)	In O ₂ -enriched air conditions, membrane separation systems are also promising alternatives to conventional CO ₂ capture methods for enriched CO ₂ flue gas deriving from power plants.
(Granados et al., 2011) (Huang et al., 2012)	CO ₂ purification and compression process using cryogenic separation is also an interesting option in partial oxy-fuel conditions. Since partial oxy-combustion leads to higher temperatures in comparison to conventional combustions, in order to maintain a boiler heat transfer profile similar to the one in air-blown boilers, and in order to control the flame temperature, flue gas recirculation had to be applied.
(Doukelis et al., 2009) (Smart and Riley, 2012) (Adeosun et al., 2013)	ECO-SCRUB Project has shown at pilot-scale that O ₂ -enriched air combustion is a technically and economically viable option for carbon capture for existing power plants leading to an energetic benefit for the overall process.
(Li et al., 2013) (Ortiz et al., 2017)	It was shown for different PZ-based solvents that the CO ₂ -loading capacities increase with increasing the CO ₂ partial pressure. Combining partial oxyfuel-conditions with a calcium looping CO ₂ capture process has also a potential for further reducing the CO ₂ capture costs in comparison with both separate technologies (oxyfuel or calcium looping).
(Cau et al., 2018)	Conventional coal-fired power plants with full and partial oxy-combustion units were compared through a detailed technico-economic assessment. Considering MEA 30 wt.%, the decrease of the CO ₂ capture energy consumption with partial oxy-fuel conditions was confirmed even if it does not compensate the costs linked to ASU for O ₂ production. Further works is needed with other solvents.
(Vega et al., 2013) (Vega et al., 2014) (Vega et al., 2016) (Vega et al., 2018) (Vega et al., 2019)	Energetic advantages (from 30% to 57% reduction of regeneration energy) thanks to partial oxy-fuel combustion conditions was confirmed with MEA and other amine-based solvents. For example, the CO ₂ absorption capacity for tertiary amines was doubled when the CO ₂ content of the flue gas reaches 60 vol.%.

recirculation of the flue gas and completed with an amine-based CO₂ capture system, was used to assess both the flexibility of the process and the performances of the solvent. The ECO-SCRUB project demonstrated that oxygen enriched air combustion is technically and economically a viable option for carbon capture and storage for existing power plants producing CO₂ enriched flue gas that will have an energetic benefit for the overall process. Nevertheless, other studies such as the one performed by (Cau et al., 2018), tend to suggest that the decrease of the CO₂ capture energy consumption thanks to partial oxy-fuel conditions does not compensate the costs linked to the Air Separation Unit used for the O₂ production. (Cau et al., 2018) indicates that potential further works should be focused on other solvents than MEA 30 wt.%.

The different works performed by Vega and co-workers (Vega et al., 2013, 2014; Vega et al., 2016, 2018; Vega et al., 2019) on CO₂ capture

applied to flue gases coming from partial oxyfuel combustion plants must also be underlined. Indeed, Vega and co-workers pointed out the energetic advantages of working with post-combustion capture using chemical absorption with amine(s)-based solvents applied to partial oxy-fuel combustion conditions. Among the different studies carried out, it was shown that the energy consumption related to solvent regeneration can reach 30% to 57% of reduction when using partial oxy-fuel combustion technology in comparison with post-combustion capture based on chemical absorption using conventional MEA 30 wt.%. The decrease of the energy consumption was also highlighted with different solvents (e.g. AMP, PZ, etc.) and the hybrid technology combining partial O₂-combustion and post-combustion CO₂ capture could be considered as a technically and economically viable technology that is able to reduce the CO₂ capture cost in large combustion facilities.

In this context, as there is still a lack of information regarding the interest of applying partial O₂-conditions to other industrial units than power plants, the main purpose of the present work was to evaluate, specifically for the cement industry case, the energetic and economical interest of applying the post-combustion CO₂ capture technology to high CO₂ concentrated flue gases, representative of partial oxy-fuel cement plant conditions. A possible implementation of such process in a cement plant is illustrated in the Supporting Information, and comparisons with other CO₂ capture technologies applied to cement plants were also performed in the CEMCAP European Project, such as in the works of (Gardarsdottir et al., 2019) and (Voldsund et al., 2019).

Moreover, the literature review presented in Table 1 also pointed out that only a few studies consider several potential solvents for the CO₂ capture process applied in such conditions. Therefore, different amine(s)-based solvents were investigated in the present study in order to confirm the interest of partial oxy-fuel conditions not only for MEA 30 wt.%, but also for other amines and blends, considering different CO₂ concentrations in the gas to treat (between 20 and 60 vol.%).

This paper will therefore expose in a first step the results of micro-pilot scale experiments and simulations (using Aspen Hysys™ V10.0) for selected solvents, based on preliminary experimental tests conducted at laboratory scale (detailed in the Supporting Information). This step was particularly important in order to validate the simulation models implemented in Aspen Hysys™ V10.0 software, such validation being not explicitly available in the literature (see in Table 1). In a second step, using a validated modeling, and considering flue gases representative of a conventional cement plant (namely Norcem Brevik in Norway) and partial oxy-fuel cement plants (simulated compositions provided by the European Cement Research Academy (ECRA)), a comprehensive comparison between conventional and partial oxyfuel conditions will be performed, including data in relation with both regeneration energies, equivalent works and operating expenses (OPEX), relevant indicators which are also innovative in comparison with available data in literature, especially for other solvents than MEA 30 wt.%.

2. Methodology, experimental devices and modeling

2.1. Selection of amines evaluated

In the case of CO₂ absorption by amine(s)-based solvents, many factors have an important influence on the selection of the solvent (CO₂ absorption capacity, kinetics of the CO₂-amine reaction, solvent regeneration energy, corrosivity, availability, degradation, etc.). Hence, the methodology of choice of the different types of amines used in this work (Dubois, 2013) based on these different criteria led to the selection presented in Table 2.

The CO₂ absorption performances with different types of simple amine aqueous solutions such as MEA (reference solvent, used at industrial scale (Knudsen et al., 2009; Raynal et al., 2011)), DEA, MDEA, AMP (conventionally 30 wt.% in aqueous solution, except for PZ due to its limited solubility into water) were tested.

Besides, in order to improve the absorption-regeneration characteristics of the amines, some amine blends are known to improve CO₂ absorption performance by combining interesting properties, i.e. good

reaction kinetics of primary and secondary amines with the high absorption capacity of tertiary or sterically hindered amines.

Activated amines (amines blended with an activator) were therefore experimented in our case. The most commonly used activator is Piperazine (PZ), which is a cyclical diamine, but Triethylenetetramine (TETRA), which is an aliphatic amines with four amine groups blended with Tetramine isomers, was also investigated.

Our methodology was to operate a first amine solvents screening at lab scale. The summary of the most relevant results is presented in the Supporting Information which gives also the detailed experimental procedure. The “best solvents” in terms of absorption performances have been selected for the micro-pilot scale tests and the results are discussed in this paper.

2.2. Absorption-regeneration micro-pilot unit

The absorption performances for amines selected after the first screening phase were tested in an absorption-regeneration micro-pilot unit in order to compare their CO₂ capture performances but also their regeneration energy. The experimental device (Fig. 1) comprises two stainless steel columns (inside diameter of 56 mm and easily adjustable packing height (H_p) of 0.5 m or 1 m packed with glass Raschig rings (6 x 6 mm)).

The incoming gas at atmospheric pressure contains N₂ and CO₂ whose respective flow rate are measured and controlled by volumetric flow regulator. The two gases are mixed together before being humidified by bubbling in water at 40 °C. After humidification, the gas flow enters the absorption column where the counter-current contact with the absorption solution takes place at atmospheric pressure. The resulting CO₂-rich loaded solution at the outlet of the absorption column is then pumped through the internal heat exchanger allowing a heat recovery, from the CO₂-lean loaded solution coming from the regeneration column to the CO₂-rich loaded solution, flowing counter-currently. After this first preheating of the solution to be regenerated, to adjust the solvent temperature at the inlet of the stripper, the CO₂-rich loaded solution is sent to a preheater (maximum heating power of 1 kW). The solution is then fed into the regeneration column equipped of a boiler (maximum heating power of 2 kW) at its bottom, which generates a concentrated CO₂ flow (sent to the hood, from the top of the column) by heating the solution up to its boiling point (e.g. T_{boiler} = 103 °C for MEA 30 wt.%). The water vapor produced is condensed and reinjected at the top of the stripping column. The consequently regenerated solvent (CO₂-lean loaded solution) is pumped back successively through the internal heat exchanger and a second heat exchanger (water cooler) allowing to lower the temperature of the solution to the absorption test temperature (40 °C), just before its entrance in the absorption column. Rotameters measure the gaseous and liquid flow rates and the differential pressure transmitters allow checking the pressure drops in the two columns. The design characteristics and operating conditions fixed for the absorption-regeneration tests are summarized in Table 3.

The unit is instrumented and completely automated in order to obtain a temporal data acquisition from all the sensors (temperature, pressure, etc.) as well as from gas analyzers and from regulators

Table 2
Amines (aqueous solutions) investigated during the absorption-regeneration tests.

Amine name	Abbreviation	Amine type	CAS number
Monoethanolamine	MEA	primary alkanolamine	141-43-5
Diethanolamine	DEA	secondary alkanolamine	111-42-2
N-methyldiethanolamine	MDEA	tertiary alkanolamine	105-59-9
2-amino-2-methyl-1-propanol	AMP	sterically hindered alkanolamine	124-68-5
2-amino-2-hydroxymethyl-1,3 propanediol	AHPD	sterically hindered alkanolamine	77-86-1
Triethylenetetramine	TETRA	Tetramine	112-24-3
Piperazine	PZ	cyclical di-amine	110-85-0

2.3.2. Liquid phase analyses

Liquid samples are collected from the installations in order to perform offline liquid analyses by quantifying the pH and CO₂ loading of the solution. The CO₂ loading representing the quantity of CO₂ that has been absorbed by a mole of amine, namely α_{CO_2} (mol CO₂/mol amine), is quantified and can be determined for the absorption test:

$$\alpha_{\text{CO}_2} = \frac{C_{\text{CO}_2}}{C_{\text{amine}}} \quad (3)$$

where C_{CO₂} is the amount of CO₂ absorbed by the solution (present in different forms: dissolved CO₂, carbonates and carbamates), measured by Total Organic Carbon analyzes (TOC-VCSH Shimadzu Analyzer) and C_{amine} is the concentration of the unloaded fresh amine solution at the beginning of the test.

More details regarding gaseous and liquid analyses are also provided in the Supporting Information.

2.4. Simulation of the absorption-regeneration process in Aspen Hysys™ software

In this section, two scales of simulations of the absorption-regeneration process will be described: (i) first of all a comparison between the experimental and simulation results of the micro-pilot unit, in order to validate the simulation model; (ii) secondly, a simulation of the CO₂ capture process in an industrial pilot plant, in order to obtain realistic regeneration energy values, representative to what would be expected in case of industrial application.

The modeling was developed in Aspen Hysys™V10.0 software using the Acid Gas Package. The package includes the physicochemical properties of acid gases, water and amines, and it takes into account appropriate thermodynamic models (e.g. Electrolyte Non-Random Two-Liquid (e-NRTL) activity coefficient for the liquid phase (Song and Chen, 2009) and fugacity coefficient for gas and vapor phases (e.g. Peng-Robinson equation of state), relevant rate-based calculation models (Zhang et al., 2009). For both cases, based on the screening tests performed at lab and micro-pilot scales, the solvents selected for the simulations were MEA (reference solvent), PZ and DEA + PZ, which are available in Aspen Hysys™V10.0 databanks. The reactions implemented in the software for these solvents are listed in Table 4.

The flowsheet developed (for both scales of simulations) in Aspen Hysys™ is illustrated on Fig. 2.

Note that a specific unit is used to perform a makeup of water and amine in order to keep the total liquid flow rate to a fixed value, to maintain the desired amine(s) concentration(s) and therefore to

compensate the possible amines and water losses at the columns outlet.

3. Results of the solvents screening and simulations

3.1. Results of the micro-pilot scale screening of simple and activated solvents

In order to carry out a comparison of the solvents performances on a common basis, the following values of the liquid flow rates were fixed for all the solvents taking into account density corrections: 7.8 l/h, 13.6 l/h and 18.4 l/h for respectively $y_{\text{CO}_2, \text{in}} = 20\%$, 40% and 60%. These values, associated to each CO₂ content in the gas to treat, were determined using preliminary Aspen Hysys™ V10.0 simulations, using the reference solvent MEA 30 wt.% and also PZ 10 wt.%.

The solvents selected for these tests were based on tests conducted at laboratory scale (given in the Supporting Information), namely: MEA, which is still commonly taken as benchmark for comparing CO₂ capture performances; PZ, which is a simple amine-based solvent showing good CO₂ absorption performances; TETRA, whose absorption performances were also close to MEA ones, and PZ-based blends with DEA or AMP, which were the activated solutions leading to the highest CO₂ capture performances.

The results of the whole screening of simple and activated solvents achieved in the micro-pilot unit are listed in Table 5 for the steady-state performances.

The interest of the absorption-regeneration micro-pilot tests was obviously to investigate the effect on the CO₂ absorption-regeneration performances of increasing $y_{\text{CO}_2, \text{in}}$ (representative of partial oxy-fuel conditions considered in the present work), but also to classify the solvents in terms of regeneration energies and absorption performances. This classification is expected to be transposable to an industrial scale (results of section 3.3 will give estimations of the solvents regeneration energies at an industrial scale). Therefore, to classify these solvents at the micro-pilot scale, MEA 30 wt.% at $y_{\text{CO}_2, \text{in}} = 20\%$ has been selected as reference case to all regeneration energies, which have been calculated using gaseous analyses (see equation (2)) and normalized to this reference.

Note that in order to check the consistency of the tests in terms of CO₂ transferred from the gas phase to the liquid phase, and corresponding to the amount of CO₂ released during the regeneration phase, balance calculations from both liquid and gas phases have been successfully conducted for the reference solvent MEA 30 wt.% even if naturally some discrepancies could exist due to the accuracy difference between the measurement methods of both phases.

Table 4
Reactions included in Aspen Hysys™V10.0 Acid Gas Package for MEA, PZ and DEA + PZ solvents reacting with CO₂.

Category	N°	Reaction	Type
Water related	(1)	$2\text{H}_2\text{O} \leftrightarrow \text{H}_3\text{O}^+ + \text{OH}^-$	Equilibrium
CO ₂ related	(2)	$\text{H}_2\text{O} + \text{HCO}_3^- \leftrightarrow \text{H}_3\text{O}^+ + \text{CO}_3^{2-}$	Equilibrium
	(3)	$\text{CO}_2 + \text{OH}^- \rightarrow \text{HCO}_3^-$	Kinetic
	(4)	$\text{HCO}_3^- \rightarrow \text{CO}_2 + \text{OH}^-$	Kinetic
MEA related (HO(CH ₂) ₂ NH ₂)	(5)	$\text{HO}(\text{CH}_2)_2\text{H}^+\text{NH}_2 + \text{H}_2\text{O} \leftrightarrow \text{HO}(\text{CH}_2)_2\text{NH}_2 + \text{H}_3\text{O}^+$	Equilibrium
	(6)	$\text{HO}(\text{CH}_2)_2\text{NH}_2 + \text{H}_2\text{O} + \text{CO}_2 \rightarrow \text{HO}(\text{CH}_2)_2\text{NHCOO}^- + \text{H}_3\text{O}^+$	Kinetic
	(7)	$\text{HO}(\text{CH}_2)_2\text{NHCOO}^- + \text{H}_3\text{O}^+ \rightarrow \text{HO}(\text{CH}_2)_2\text{NH}_2 + \text{H}_2\text{O} + \text{CO}_2$	Kinetic
PZ related (C ₄ H ₈ (NH) ₂)	(8)	$\text{C}_4\text{H}_8(\text{NH})_2 + \text{H}_3\text{O}^+ \leftrightarrow \text{C}_4\text{H}_8(\text{NH})_2\text{H}^+ + \text{H}_2\text{O}$	Equilibrium
	(9)	$\text{H}_2\text{O} \leftrightarrow \text{C}_4\text{H}_8(\text{NH})_2\text{COO}^- + \text{H}_3\text{O}^+$	Equilibrium
	(10)	$\text{C}_4\text{H}_8(\text{NH})_2 + \text{H}_2\text{O} + \text{CO}_2 \rightarrow \text{C}_4\text{H}_8(\text{NH})\text{NCOO}^- + \text{H}_3\text{O}^+$	Kinetic
	(11)	$\text{C}_4\text{H}_8(\text{NH})\text{NCOO}^- + \text{H}_3\text{O}^+ \rightarrow \text{C}_4\text{H}_8(\text{NH})_2 + \text{H}_2\text{O} + \text{CO}_2$	Kinetic
	(12)	$\text{C}_4\text{H}_8(\text{NH})\text{NCOO}^- + \text{H}_2\text{O} + \text{CO}_2 \rightarrow \text{C}_4\text{H}_8(\text{NCOO}^-)_2 + \text{H}_3\text{O}^+$	Kinetic
	(13)	$\text{C}_4\text{H}_8(\text{NCOO}^-)_2 + \text{H}_3\text{O}^+ \rightarrow \text{C}_4\text{H}_8(\text{NH})\text{NCOO}^- + \text{H}_2\text{O} + \text{CO}_2$	Kinetic
DEA related (HO(CH ₂) ₂ NH(CH ₂) ₂ OH)	(14)	$\text{HO}(\text{CH}_2)_2\text{NH}_2^+(\text{CH}_2)_2\text{OH} + \text{H}_2\text{O} \leftrightarrow \text{HO}(\text{CH}_2)_2\text{NH}(\text{CH}_2)_2\text{OH} + \text{H}_3\text{O}^+$	Equilibrium
	(15)	$\text{HO}(\text{CH}_2)_2\text{NH}(\text{CH}_2)_2\text{OH} + \text{H}_2\text{O} + \text{CO}_2 \rightarrow \text{HO}(\text{CH}_2)_2\text{N}(\text{CH}_2)_2\text{OHCOO}^- + \text{H}_3\text{O}^+$	Kinetic
	(16)	$\text{HO}(\text{CH}_2)_2\text{N}(\text{CH}_2)_2\text{OHCOO}^- + \text{H}_3\text{O}^+ \rightarrow \text{HO}(\text{CH}_2)_2\text{NH}(\text{CH}_2)_2\text{OH} + \text{H}_2\text{O} + \text{CO}_2$	Kinetic

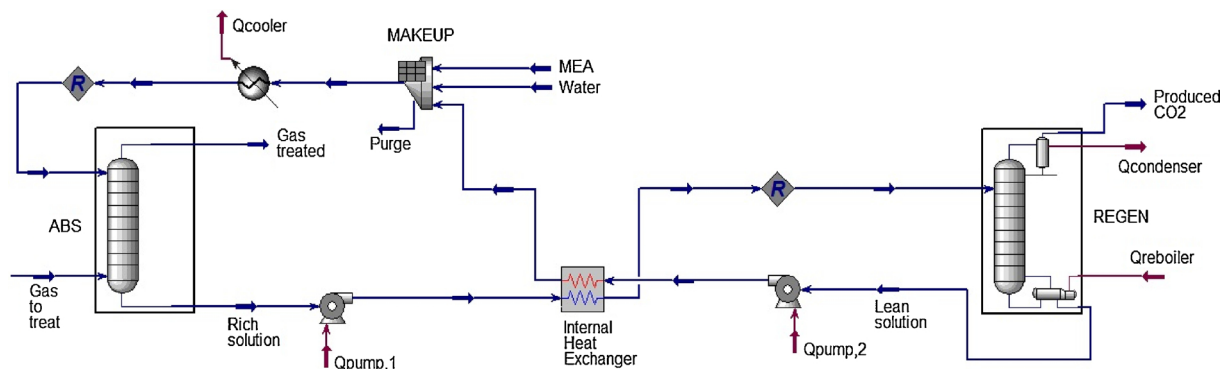


Fig. 2. Aspen Hysys™ flow sheet for the conventional MEA process configuration.

It can be noted that the CO₂ deriving from the absorption-regeneration process in the micro-pilot unit is produced with a purity (Y_{CO₂,regen}) of over 92% for all the solvents. The purpose of our solvents screening at micro-pilot-scale is clearly to identify the solvent(s) likely to maximize the absorption ratio and minimize the regeneration energy. We can see from Table 5 that the best absorption performances in the range of tested CO₂ inlet concentration (20% to 60%), were obtained with the activated solutions DEA 30 wt.% + PZ 5 wt.% (A ≈ 89–91%) and AMP 30 wt.% + PZ 5 wt.% (A ≈ 91–98%). Regarding PZ solution, it must be noted that the concentration was limited to 10 wt.% in order to stay under the solubility limit (around 15 wt.% in our operating conditions). Higher PZ concentrations (e.g. 40 wt.%, such as in the works of (Van Der Ham et al., 2014; Freeman et al., 2009)) are possible at industrial scale thanks to higher operating pressure, temperature and solvent CO₂ loading. Together with these measured absorption performances, the regeneration energy was assessed for each solvent (eq. (2)). The absolute values of the energies of regenerations relative to MEA 30 wt.% and for all solvents tested are listed in Table 5. Fig. 3 represents the evolution and comparison of the relative regeneration energies characterizing the solvents screened at different CO₂ contents in the gas to treat.

A significant global conclusion could be drawn from Fig. 3: when increasing the CO₂ content in the gas to treat from 20% to 60%, lower regeneration energies are required by all the solvents, especially for the activated solutions DEA 30 wt.% + PZ 5 wt.% and AMP 30 wt.% + PZ 5 wt.%. Indeed, when the CO₂ concentration in the flue gas increases, the CO₂ regenerated (or absorbed) molar flow increases. Since P_{boiler} is fixed, the energy of regeneration will decrease as inversely proportional

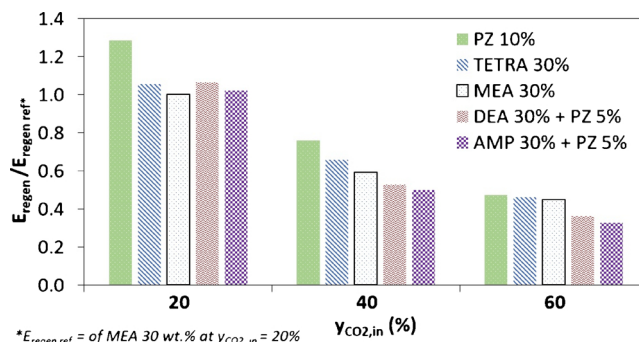


Fig. 3. Regeneration energies of the different solvents tested at micro-pilot scale (Y_{CO₂,in} = 20%, 40% and 60%) relatively to E_{regen} of MEA 30 wt.% at Y_{CO₂,in} = 20%.

to the quantity of CO₂ absorbed (equation (2)). Accordingly, among the solvents tested, the best characteristics maximizing the absorption ratio and minimizing the required regeneration energy are obtained mainly for DEA 30 wt.% activated with PZ 5 wt.% and AMP 30 wt.% activated with PZ 5 wt.%.

Globally, the observations performed from Fig. 3 confirm that increasing the CO₂ content in the gas to treat, thanks to the implementation of partial oxyfuel combustion in cement plants, tends to lower the solvent regeneration energy. The purpose of the next sections will be to confirm and complete these conclusions (including equivalent works and OPEX comparisons) but at an industrial scale. For carrying out these analyses,

Table 5
Main results of the micro-pilot scale absorption-regeneration tests.

	C _{amine} (mol/l)	Y _{CO₂, in} (%)	L _{lean} (L/h)	A (%)	E _{regen} /E _{regen MEA 30 wt.%} (at Y _{CO₂ = 20%)}	α _{rich} (mol CO ₂ /mol amine)	α _{lean} (mol CO ₂ /mol amine)	Δα (mol CO ₂ /mol amine)
MEA 30 wt.%	4.94	20	7.76	94	1.00	0.37	0.12	0.25
	4.85	30	10.68	92	0.69	0.40	0.23	0.17
	5.12	40	13.59	80	0.59	0.40	0.22	0.18
	5.11	50	15.53	80	0.47	0.33	0.15	0.18
	5.09	60	18.44	69	0.45	0.40	0.23	0.17
PZ 10 wt.%	1.40	20	7.76	73	1.29	0.64	0.13	0.52
	1.11	40	13.59	63	0.76	1.20	0.73	0.47
	1.14	60	18.44	68	0.47	0.99	0.41	0.58
TETRA 30 wt.%	2.17	20	7.76	92	1.06	0.71	0.31	0.40
	2.12	40	13.59	72	0.66	1.20	0.64	0.56
	2.18	60	18.44	69	0.46	0.71	0.33	0.38
AMP 30 wt.% + PZ 5 wt.%	4.17	20	7.76	91	1.02	0.52	0.26	0.26
	4.00	40	13.59	97	0.50	0.49	0.26	0.23
	4.15	60	18.44	98	0.33	0.39	0.18	0.21
DEA 30 wt.% + PZ 5 wt.%	3.61	20	7.76	91	1.06	0.52	0.26	0.26
	3.65	40	13.59	91	0.53	0.44	0.22	0.22
	3.70	60	18.44	89	0.36	0.45	0.18	0.27

the Aspen Hysys™ simulations will be carried out for three selected solvents (namely MEA, PZ and DEA + PZ) and firstly validated with our micro-pilot experimental results (in section 3.2) before being applied to simulate a process at a higher scale (in section 3.3).

3.2. Simulation of the absorption-regeneration micro-pilot unit: comparison between experimental and simulations results

The absorption-regeneration tests previously conducted in the micro-pilot unit were simulated for MEA 30 wt.%, PZ 10 wt.% and the blend DEA 30 wt.% + PZ 5 wt.% fixing the same operating conditions as the experimental tests (see Table 3). The dimensional parameters used in these simulations are given in section 2.3. The flowsheet considered and the modeling parameters are given in section 2.4.

The comparisons of the experimental and simulation results relative to the regeneration energy for MEA, PZ and the blend DEA + PZ are presented on Fig. 4 for a range of $y_{CO_2,in}$ from 20% to 60%. The first conclusion driven from the analysis of Fig. 4 is that for the three solvents, the simulated regeneration energies have very similar trends to the experimental ones. Consequently, the model seems to predict well the results for MEA 30 wt.%, PZ 10 wt.% and DEA 30 wt.% + PZ 5 wt.% simulations.

The second conclusion confirms the experimental observation relative to the micro-pilot unit (Fig. 3): when the CO_2 content in the gas to treat is increased, the regeneration energies of the solvents advantageously decrease. The comparisons of the experimental and simulation results relative to the absorption ratios for the three solvents are given in Fig. 5.

It can be deduced from Fig. 5 that for the three solvents, the same tendency was shown for experimental and simulation results. The average absorption ratios of MEA 30 wt.% relative to the experimental and simulation results were 83% and 86% respectively. Considering PZ 10 wt.%, lower absorption ratios (averages) of 68% for the experimental and 67% for the simulation results were obtained. The highest absorption ratios were observed with the blend DEA 30 wt.% + PZ 5 wt.% corresponding to 90% for the experimental and 88% for the simulation results.

The simulation model used to assess the regeneration energy relative to the absorption-regeneration process in amine-based solvents was therefore validated at micro-pilot scale. Thus, values of this energy, for the same tested solvents, were estimated for an industrial pilot scale, and completed with an analyze including calculations of equivalent works and operating expenses.

3.3. Simulation of an industrial pilot unit in Aspen Hysys™

3.3.1. Industrial simulations regarding the reference solvent MEA 30 wt. %

Regarding the installation simulated in Aspen Hysys™V10.0 software, the model was based on the an pilot installation tested previously (Knudsen et al., 2009) and for which the operating and design parameters are known, which is not possible with most of the other units. The flowsheet of the simulated unit was the same as the one presented in Fig. 2, a conventional CO_2 capture process configuration being considered in the present case.

This pilot is sized to handle a gas flow of 4000 m^3/h at the inlet of the absorber after removal of a large quantity of water, cooling and compression. The liquid flow rate is equal to 22 m^3/h as base case. Among the other parameters imposed in the simulation, it must be pointed out the purity of the CO_2 recovered, fixed at a classical value of 98 mol.% (Hassan, 2005). Design information regarding the absorption and regeneration columns, and the operating parameters associated, are also provided in Table 6.

Concerning the gas to treat, the flue gas composition for the base case ($y_{CO_2,in}$ around 20%) was based on the Brevik cement plant flue gas in Norway, which is initially at 165 °C and 100 kPa prior to compression to 120 kPa and cooling down to 40 °C before entering the absorber (see conditioned gas composition in Table 7).

Other compositions with higher CO_2 contents in the gas to treat (indicated in Table 7) were based on simulations carried out in collaboration with ECRA of a 3000 $t_{clinker}/day$ cement plant with an oxygen demand fixed to 0.15 $m^3/kg_{clinker}$ (standard conditions of pressure and temperature).

Note that in the present case, SO_x and NO_x concentrations were not considered. More precisely, by varying the air input into the kiln and consequently the recycle ratio, different compositions (partial oxy-fuel conditions) of extracted flue gas to post-combustion plant could be obtained, leading to the different $y_{CO_2,in}$ values of Table 7. For each case presented in Table 7, parametric studies were performed and different scenarios were considered in order to identify the optimized operating parameters (see (Dubois et al., 2017) for more details on considered scenarios). The scenario allowing to minimize the regeneration energy has been selected to compare the results for the three solvents: MEA, PZ and DEA + PZ. Consequently, for the simulations, instead of fixing the absorption ratio for all cases, the amount of CO_2 produced at the outlet of the stripper ($y_{CO_2,abs}$) was maintained at 1.5 t_{CO_2}/h , corresponding to an absorption rate of 90% for $y_{CO_2,in}$ equal to 20%. The liquid flow rate was adjusted in order to minimize E_{regen} for an inlet CO_2 content of the gas to treat equal to 20% ($L = 22 m^3/h$). The detailed simulation results for different CO_2 contents in the gases to treat are presented in Table 8.

In the context of Carbon Capture and Utilization, this approach of fixing the recovered CO_2 amount has the advantage that the results can be transposed and compared in terms of same amount of “final CO_2 -based product” (e.g. methanol), the disadvantage being that the relative quantity of captured CO_2 (absorption ratio) is decreased when $y_{CO_2,in}$ is increased. Nevertheless, two important points must be highlighted. First of all, as shown in other studies (see bibliographic review in Table 1, especially the results from the ECO-SCRUB European Project) and also in our previous works (e.g. (Dubois et al., 2017)), this decrease of E_{regen} with higher $y_{CO_2,in}$ values could be also pointed out with a constant absorption ratio (e.g. 90%) approach. The second point is the fact that comparing results at different CO_2 absorption ratio values was also performed and validated in other projects (see for example the works of (Biermann et al., 2018) on “partial carbon-capture”), especially to highlight that capturing CO_2 at a lower absorption ratio leads to an economic benefit (e.g. (Biermann et al., 2018) show a decrease of specific CO_2 capture costs when the CO_2 content in the gas to treat is increased from 5 vol.% to 30 vol.% with a CO_2 absorption ratio decreasing from 90% to 67% and 47%).

Based on these simulation results presented in Table 8, it can be observed that consistent orders of magnitude of E_{regen} are obtained. Indeed, according to (Zhang et al., 2016), for a benchmark MEA based capture system, a value of 3–4 GJ/t_{CO_2} can be considered as the average energy requirement and according to (Hills et al., 2016), the thermal energy demand of amine scrubbing is at least 2 GJ/t_{CO_2} . Another observation that can be drawn is the fact that higher $y_{CO_2,in}$ values induce higher solvent CO_2 loadings, especially for the lean solution.

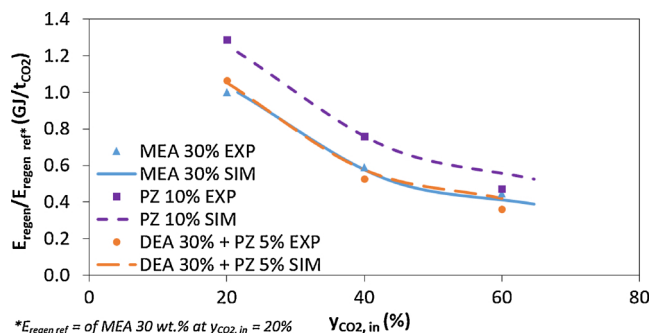


Fig. 4. Comparison of experimental and simulated regeneration energies of MEA 30 wt.%, PZ 10 wt.% and DEA 30 wt.% + PZ 5 wt.% ($y_{CO_2,in} = 20\%$, 40% and 60%) relative to the experimental value E_{regen} of MEA 30 wt.% at $y_{CO_2,in} = 20\%$.

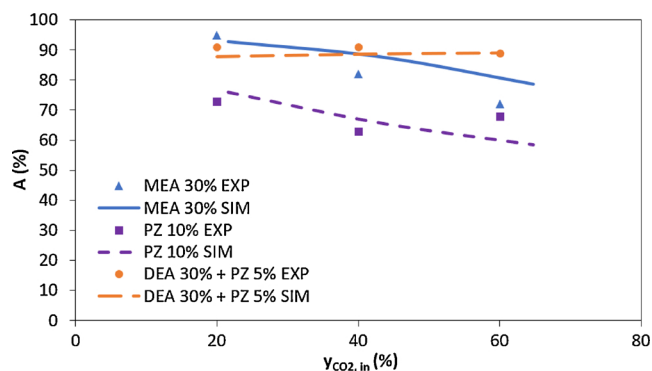


Fig. 5. Comparison of experimental and simulated absorption ratios of MEA 30 wt.%, PZ 10 wt.% and DEA 30 wt.% + PZ 5 wt.% ($Y_{CO_2,in} = 20\%$, 40% and 60%).

Table 6

Dimensions and operating conditions for the two columns.

	Absorber	Stripper
Column Diameter (m)	1.1	1.1
Packing height (m)	17 (17 x 1 m)	10 (10 x 1 m)
Packing type	Random packing IMTP	Random packing IMTP
	50	50
Inlet liquid temperature (°C)	40	110
Bottom pressure (kPa)	120	200
Linear pressure drop (kPa/m)	0.5	0.5

Table 7

Compositions (in mol fractions) of the gas to treat after conditioning.

Component (mol. fract.)	Conventional combustion (Brevik's cement data)	Partial oxy-fuel combustion (ECRA simulations)			
		Base case	Case 1	Case 2	Case 3
N ₂	0.647	0.575	0.488	0.399	0.281
CO ₂	0.204	0.310	0.441	0.514	0.620
H ₂ O	0.062	0.062	0.048	0.056	0.062
O ₂	0.086	0.053	0.023	0.031	0.037

Table 8

Aspen Hysys™ simulation results with MEA 30 wt.% for different compositions of the gases to treat (L = 22 m³/h and G = 4000 m³/h).

	Base case	Case 1	Case 2	Case 3	Case 4
$Y_{CO_2,in}$ (%)	20.40	31.00	44.10	51.44	62.03
A (%)	90.00	56.49	38.31	29.32	26.32
E_{regen} (GJ/ t CO ₂)	3.36	2.86	2.48	2.39	2.11
E_{regen} saving / base case (%)		14.88	26.19	28.87	37.20
$\alpha_{CO_2,rich}$ (mol CO ₂ /mol MEA)	0.51	0.55	0.57	0.58	0.59
$\alpha_{CO_2,lean}$ (mol CO ₂ /mol MEA)	0.21	0.25	0.28	0.29	0.31
pH _{rich}	8.35	8.22	8.04	8.03	8.02
pH _{lean}	9.90	9.81	9.72	9.70	9.68

3.3.2. Industrial simulations regarding PZ 40 wt.% and DEA 30 wt.% + PZ 15 wt.%

Regarding the simulations with the cyclical diamine piperazine, based on (Van Der Ham et al., 2014) and (Freeman et al., 2009), the conventional concentration of this solvent is 8 M (40 wt.%). This value was fixed for the simulations. Moreover, high regeneration temperature is generally reached with such piperazine-based solvents, thus with a higher pressure (600 kPa) in the regeneration column than for MEA 30 wt.% leading to a boiler temperature of 150 °C (the absorption process being still performed at 40 °C). The interest of increasing the regeneration pressure in terms of E_{regen} , can be found in the work of

(Dubois and Thomas, 2018). Besides, for each boiler pressure, an optimized (L/G)_{vol} can be found in order to minimize the reboiler duty.

The simulation flowsheet was the one presented on Fig. 2, and the operating conditions together with the columns dimensions are listed in Table 6. The gas enters the absorber where the process takes place at 120 kPa and 40 °C but unlike for the MEA 30 wt.%, concerning PZ 40 wt.%, the solvent regeneration takes places at 600 kPa and 159 °C. The gas and liquid flow rates are fixed respectively to 4000 m³/h and 12.5 m³/h; the latter allowing minimum value of E_{regen} for $Y_{CO_2,in} = 20\%$ at (L/G)_{vol} equal to $3.16 \cdot 10^{-3}$. In the case of the industrial simulations relative to the amine blend DEA + PZ, in order to achieve the comparison between PZ 40 wt.% and the blend DEA 30 wt.% + PZ 15 wt.%, the same operating parameters (characteristics of PZ 40 wt.%) were chosen for the simulation of DEA 30 wt.% + PZ 15 wt.% (e.g. columns pressure). Besides, at industrial scale, higher PZ concentrations are used (Mudhasakul et al., 2013) (Wilck et al., 2017). In this case a concentration of 15 wt.% was chosen since it is the minimum achievable in the fixed operating conditions to reach the targeted performances, lower concentrations of PZ being not suitable due to the favorable effect of piperazine on the kinetics of absorption. The flue gas compositions taken for PZ 40 wt.% and DEA 30 wt.% + PZ 15 wt.% simulations are the ones presented in Table 7.

Tables 9 and 10 give an overview of the industrial simulations achieved for PZ 40 wt.% and for the amine blend DEA 30 wt.% + PZ 15 wt.% respectively.

As for MEA 30 wt.%, it can be seen in Table 9 for PZ 40 wt.% and in Table 10 for DEA 30 wt.% + PZ 15 wt.% that the increase of $Y_{CO_2,in}$ leads to higher CO₂ loading values.

3.3.3. Regeneration energies comparison at industrial pilot scale

Fig. 6 shows the comparison, for different CO₂ contents in the gas to treat (Table 7), of the regeneration energies calculated for the benchmark MEA 30 wt.%, for PZ 40 wt.% and the amine blend DEA 30 wt.% + PZ 15 wt.%.

The conclusions driven from the industrial pilot unit simulations using Aspen Hysys™ are the same as the ones driven from the experimental tests (Fig. 3) and the simulations (Fig. 4) relative to the absorption-regeneration micro-pilot unit. Indeed, thanks to the O₂-enriched air combustion conditions, the resultant high CO₂ contents in the gas to treat decrease beneficially the regeneration energy of the solvent when applying a CO₂ post-combustion capture by absorption-regeneration. More precisely, the results at industrial scale show that an increase of $Y_{CO_2,in}$ from 20% to 44% (case 2) leads to a decrease of 26% of the MEA 30 wt.% regeneration energy (from 3.36 to 2.48 GJ/tCO₂). When $Y_{CO_2,in}$ reaches 62% (case 4), the solvent regeneration energy is equal to 2.11 GJ/tCO₂, which means a decrease of 37% in comparison with the base case.

Even if for the base case ($Y_{CO_2,in} = 20.4\%$) E_{regen} values of PZ and DEA + PZ are lower than the one of MEA, at higher CO₂ contents in the gas to treat, the decrease of the energy of regeneration of MEA is more significant than the two other solvents (2.75 and 2.67 GJ/tCO₂ for PZ and DEA + PZ respectively, at $Y_{CO_2,in} = 62\%$).

These observations confirm that applying partial oxy-fuel conditions in the cement industry with the objective of increasing the CO₂ content

Table 9

Main results of the industrial scale simulations of PZ 40 wt.% (L = 12.5 m³/h and G = 4000 m³/h).

	Base case	Case 2	Case 4
$Y_{CO_2,in}$ (%)	20.40	44.10	62.03
A (%)	90.12	38.32	26.42
E_{regen} (GJ/ t CO ₂)	3.24	2.86	2.77
E_{regen} saving / base case (%)		11.73	14.51
$\alpha_{CO_2,rich}$ (mol CO ₂ /mol MEA)	0.74	0.82	0.86
$\alpha_{CO_2,lean}$ (mol CO ₂ /mol MEA)	0.18	0.27	0.32
pH _{rich}	8.31	8.06	7.84
pH _{lean}	10.33	10.10	9.99

Table 10

Main results of the industrial scale simulations of DEA 30 wt.% + PZ 15 wt.% ($L = 12.5 \text{ m}^3/\text{h}$ and $G = 4000 \text{ m}^3/\text{h}$).

	Base case	Case 2	Case 4
$y_{\text{CO}_2, \text{in}}$ (%)	20.40	44.10	62.03
A (%)	89.73	38.36	26.36
E_{regen} (GJ/ t CO_2)	3.03	2.73	2.67
E_{regen} saving / base case (%)		9.91	11.67
$\alpha_{\text{CO}_2, \text{rich}}$ (mol CO_2 /mol MEA)	0.61	0.67	0.70
$\alpha_{\text{CO}_2, \text{lean}}$ (mol CO_2 /mol MEA)	0.05	0.12	0.15
$p\text{H}_{\text{rich}}$	8.44	8.20	8.07
$p\text{H}_{\text{lean}}$	8.24	7.94	7.87

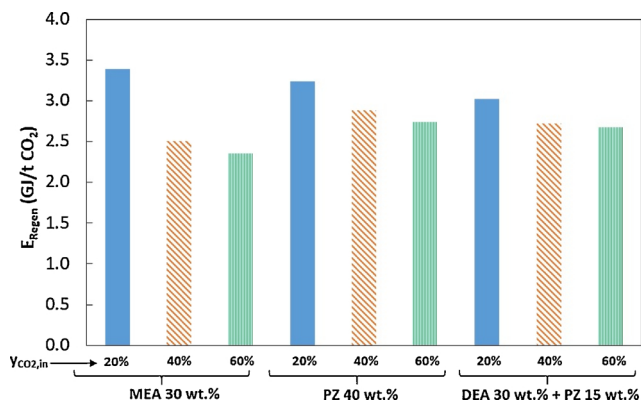


Fig. 6. Aspen Hysys™ comparison of the regeneration energies of MEA 30 wt.% ($P = 200 \text{ kPa}$), PZ 40 wt.% ($P = 600 \text{ kPa}$) and DEA 30 wt.% + PZ 15 wt.% ($P = 600 \text{ kPa}$) for different CO_2 contents in the gas to treat.

of the gas to treat is a very interesting option as the energy demand of the CO_2 capture unit is decreased. Nevertheless, other indicators have to be taken into account (equivalent work and OPEX) in order to evaluate the interest of working in partial oxy-fuel conditions.

3.3.4. Equivalent works comparison at industrial pilot scale

Even if the focus was put on minimizing E_{regen} for optimizing the operating conditions considered for the simulation cases, another indicator was also investigated, namely the total equivalent thermodynamic work (W_{equ} [GJ/t CO_2]), allowing to unify the thermal and electrical energy consumptions and which was determined using the same approach as in (Karimi et al., 2011) and (Dubois and Thomas, 2018):

$$W_{\text{equ}} = E_{\text{regen}} \left(1 - \frac{T_C + 273.15}{T_H + 273.15} \right) \eta_{\text{turbine}} + W_{\text{pumps}} + W_{\text{compressors}} \quad (4)$$

where T_C [°C] which is the condensation temperature of the steam in the power plant's turbine providing the electrical energy to the cement plant (assumed to be 40 °C), T_H [°C] which corresponds to the reboiler steam temperature (assumed to be 10 °C higher than the temperature at the reboiler, namely T_{regen}), η_{turbine} , which is the efficiency of the turbine (assumed to be 75%), W_{pumps} and $W_{\text{compressors}}$ [GJ/t CO_2] the electrical energies used to run the pumps and eventual compressors (values provided by Aspen Hysys™, more details being available in the Supporting Information). Note that in the present case, $W_{\text{compressors}}$ is equal to zero (no CO_2 compression considered and no process configuration needing compression). The comparison of W_{equ} calculated for the three solvents and for different $y_{\text{CO}_2, \text{in}}$ values is provided on Fig. 7.

Firstly, it can be highlighted from Fig. 7 that as previously seen for E_{regen} , W_{equ} is decreasing when $y_{\text{CO}_2, \text{in}}$ is increased. Nevertheless, higher W_{equ} values are observed with PZ 40 wt.% and DEA 30 wt.% + PZ 15 wt.% indicating that in such cases, the higher regeneration temperatures needing higher steam temperatures (which tend to increase W_{equ}) are not counterbalanced by eventual lower E_{regen} values.

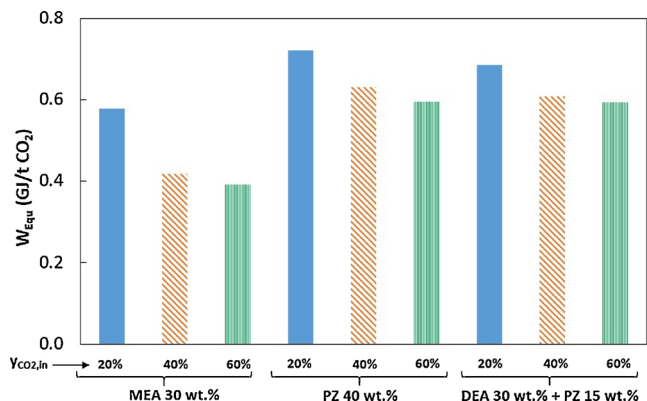


Fig. 7. Equivalent work relative to the absorption-regeneration process for MEA 30 wt.%, PZ 40 wt.% and DEA 30 wt.% + PZ 15 wt.% (at different $y_{\text{CO}_2, \text{in}}$ values).

Indeed, it is important to keep in mind that the minimized parameter is the solvent regeneration energy and not the total thermodynamic equivalent work, meaning that other conditions could potentially lead to smaller W_{equ} values. Nevertheless, as already stated in (Dubois and Thomas, 2018), such approach can be validated for the cement plant application as the electrical demands in relation with the different equipment (e.g. compressors or pumps) will potentially come from an external source, eventually a renewable one or taking advantage of excess power available. Additionally, in a cement plant, the external energy demands could be also partially offset by some thermal energy recovery (from 5% to 15% of the reboiler duty as a function of the plant).

3.3.5. OPEX evaluation of the absorption-regeneration process applied to high CO_2 concentrated flue gases

The operating costs of the industrial process relative to the three solvents tested at industrial scale (MEA 30 wt.%, PZ 40 wt.% and DEA 30 wt.% + PZ 15 wt.%) were evaluated using Aspen Economics™ module available from Aspen Hysys™ V10.0 simulations. The flowsheet, the dimensional and operating parameters were described in section 3.3. The total gas flow rate to be treated was fixed to 4000 m^3/h (6.2 $t_{\text{gas to treat}}/\text{h}$) and the CO_2 captured flow rate was also a fixed parameter, namely 1.5 $t_{\text{captured CO}_2}/\text{h}$. The details relative to the utilities costs considered for the OPEX calculations (all data being taken for the year 2016) are listed in Table 11.

The equation 4 was used to calculate the OPEX (in €/t captured CO_2) for each utility presented in Table 11.

$$\text{OPEX}_U = \frac{\text{Cost}_U \times \text{Consumption}_U}{\text{Captured CO}_2 \text{ flow rate} \left(\frac{t_{\text{captured CO}_2}}{h} \right)} \quad (5)$$

OPEX_U corresponding to the operating expenditures in relation with the utility U (namely electricity, steam and cooling water), in €/t captured CO_2 U is the cost of the utility in €/MWh (electricity) or €/t (others), and Consumption_U is the consumption of the utility U in MW or in t/h.

The detailed costs of the utilities and the corresponding total OPEX (€/t captured CO_2) for MEA 30 wt.%, PZ 40 wt.% and DEA 30 wt.% + PZ 15 wt.% were determined for different CO_2 contents in the gas to treat and are represented on Fig. 8.

For the three solvents considered, the operating expenses decrease when increasing the CO_2 content in the gas to treat. More precisely, the solvent MEA 30 wt.% shows a decrease of 28% in the OPEX when increasing

$y_{\text{CO}_2, \text{in}}$ from 20% (total OPEX ≈ 75 €/t captured CO_2) to 60% (total OPEX ≈ 54 €/t captured CO_2). In the same conditions, reductions of 23% and 22% were observed for PZ wt.% and DEA 30 wt.% + PZ 15 wt.%

Table 11
Utilities costs taken for OPEX calculations.

Utilities	Costs
Electricity	50 €/MWh (based on 2016 average electricity costs (European Commission, 2017))
Fresh water	0.30 €/t fresh water (Li et al., 2016)
Steam	28.22 €/ton of steam* (Sun et al., 2016)
Total treated CO ₂ flow rate	1.5 t _{treated CO₂} /h

* Conversion rate conversion in September 2018: 1 US \$ is equal to 0.85 €.

respectively. Analyzing more deeply the results presented on Fig. 8, it can be seen that quite logically, the main contribution to OPEX costs is linked to the steam needed to perform the solvents regeneration, which represents from 60% to 65% of the total OPEX for MEA 30 wt.%, 80% to 90% of the total OPEX for PZ 40 wt.% and from 75% to 80% of the total OPEX for DEA 30 wt.% + PZ 15 wt.%.

The evolution of the steam demand as a function of $y_{CO_2,in}$ can be directly put in parallel of the E_{regen} evolutions presented on Fig. 6. Regarding the electricity demand, it represents only 2% to 4% of the total OPEX in all cases. Concerning the cooling water demand, it can be pointed out from Fig. 8 that it is relatively more significant in the case of MEA 30 wt.% (representing around 35% of the total OPEX) than with other solvents (representing from 7% to 25% of the total OPEX depending on the case considered).

Globally, in all cases, PZ-based solvents lead to lower OPEX than MEA 30 wt.%, with a lowest value of OPEX obtained in the case of DEA 30 wt.% + PZ 15 wt.% at $y_{CO_2,in} = 60\%$, namely 45 €/t_{captured CO₂}. This is an important observation because as seen in previous sections, this is not necessarily the case when E_{regen} or W_{equ} are compared. Moreover, considering that according to literature (IEAGHG, 2008), the benchmark for the cost of CO₂ post-combustion capture applied to fumes coming from a conventional combustion is about 60 €/t_{captured CO₂}, the interest of applying partial oxyfuel combustion is confirmed.

Nevertheless, even if the interest of considering partial oxy-fuel combustion for the cement industry exhaust gases was proved here to be cost-favorable, it is important to assess the cost necessary for oxygen production in the air separation unit needed to enrich the air combustion with oxygen. For this purpose, in order to complete the cost analyses performed in the present work, preliminary calculations have been made for a real plant capturing CO₂, (see for example Saskpower Boundary Dam power plant among different industrial units presented in (Idem et al., 2015)) which capture capacity would be equal to 3300 t_{CO₂}/day. The cost of Cryogenic O₂ separation (purity of 99%) can be considered between 15 and 28 €/t_{O₂} (CEMCAP-SINTEF-ER, 2017), leading to a cost of oxygen production between 0.40 - 0.74 €/t_{captured CO₂} for $y_{CO_2,in} = 40\%$ and between 1.95–3.64 €/t_{captured CO₂} for $y_{CO_2,in} = 60\%$. Therefore, even if in a first simplified approach, such costs were added to the total OPEX previously detailed (45 €/t_{captured CO₂} in the best case), the economic interest of implementing partial oxyfuel could still be confirmed.

4. Conclusions and prospects

The present work was focused on an innovative CO₂ capture technique called the post-combustion capture applied to a partial oxy-fuel combustion (O₂-enriched air combustion) dedicated to cement industry. This technology combines an O₂-enriched air combustion involving a more CO₂-concentrated flue gas (between 20% and 60%) compared to a conventional combustion and allowing the application of a CO₂ post-combustion capture using amine(s)-based solvents. Indeed, thanks to a more CO₂-concentrated flue gas and the choice of an adequate solvent, this process assures a decrease of the regeneration energy in the amine plant (compared to the conventional post-combustion).

In order to study the applicability of this technology to the cement industry, different aspects were here investigated. In a first step, the performances of several solvents were evaluated thanks to tests carried out at laboratory scale considering conventional to high CO₂ contents ($y_{CO_2,in} = 20\text{--}60$ vol.%) in cement plant flue gases. Simple and activated solvents were screened in such conditions and compared. Based on the results obtained at lab scale, measurement were conducted at micro-pilot scale for the best solvents screened and results were confirmed: the use of the activated solutions of AMP or DEA with PZ 5 wt.% leads to particularly high absorption performances both in standard and high CO₂ contents conditions, the performances being higher than with conventional solvents such as MEA 30 wt.%.

In a next step of the study, simulations were conducted in Aspen Hysys™ for the micro-pilot unit for three solvents, namely: MEA 30 wt.%, PZ 10 wt.% and DEA 30 wt.% + PZ 5 wt.%. The purpose of this step was to validate the simulation model before implementing it for industrial scale simulations. An important conclusion was driven from this step: the regeneration energy for all the solvents tested decreases when the CO₂ content in the gas to treat increases.

Afterwards, in order to evaluate these energies of regeneration at a scale closer to the real application, an industrial pilot unit was simulated using the same modeling and solvents in Aspen Hysys™. The same relevant conclusion can be drawn: the regeneration energy advantageously decreases when increasing the CO₂ content in the gas to treat. The decrease of the regeneration energy of MEA from 3.36 GJ/t_{CO₂} at $y_{CO_2,in} = 20.4\%$ to 2.11 GJ/t_{CO₂} at $y_{CO_2,in} = 62\%$ (37% compared to the conventional combustion case), was more significant than for the two other solvents (2.75 and 2.67 GJ/t_{CO₂} for PZ and DEA + PZ respectively at $y_{CO_2,in} = 62\%$, corresponding to a decrease of 15% and 12% respectively). In parallel, two other parameters were also investigated, namely the operating expenses using Aspen Economics™ module and the total equivalent work, which is innovative in comparison with current available data in literature, in particular for other solvents than MEA 30 wt.%. For both indicators, the interest of increasing $y_{CO_2,in}$ was clearly shown. More particularly, regarding the OPEX, the lowest value was obtained in the case of DEA 30 wt.% + PZ 15 wt.% at $y_{CO_2,in} = 60\%$, namely 45 €/t_{captured CO₂}, showing a clear economic advantage in comparison with conventional combustion conditions, even if the oxygen production costs are taken into account (less than 4 €/t_{captured CO₂}).

Globally, to underline even more the interest of considering the absorption-regeneration CO₂ capture process applied to partial oxyfuel cement plant flue gases, further works could be carried out in order to have a more complete evaluation of this technology. For example, better solvents could be considered for future simulations (e.g. other activated solutions such as AMP + PZ whose interesting performances were also clearly identified during the experimental tests). Other process configurations, such as highlighted in (Dubois and Thomas, 2018), could be also investigated as complementary solutions to partial oxyfuel implementation in order to reduce even more the cost of the CO₂ capture process.

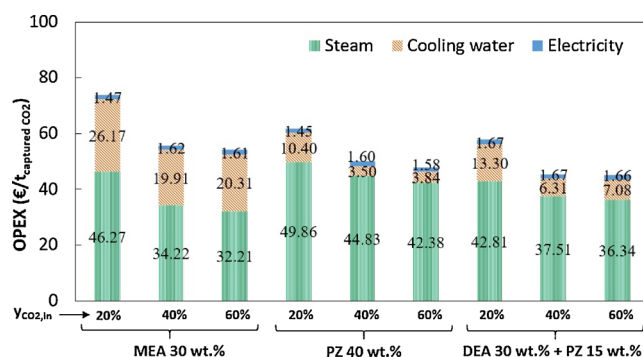


Fig. 8. OPEX relative to the absorption-regeneration process for MEA 30 wt.%, PZ 40 wt.% and DEA 30 wt.% + PZ 15 wt.% (at different $y_{CO_2,in}$ values).

Acknowledgments

European Cement Research Academy (ECRA) and HeidelbergCement Company are warmly acknowledged by the authors for their support (technical and financial) accorded to the ECRA Academic Chair at the University of Mons.

Appendix Supplementary data

Supplementary material related to this article can be found, in the online version, at doi:<https://doi.org/10.1016/j.ijggc.2019.102799>.

References

- Adeosun, A., Muthiah, A., Abu-Zahra, M.R.M., 2013. Evaluation of oxygen-enriched air combustion process integrated with CO₂ post-combustion capture. *Therm. Environ. Eng.* 5, 113–121. <https://doi.org/10.5383/ijtee.05.02.003>.
- Belaissouli, B., Le Moulec, Y., Willson, D., Favre, E., 2012. Hybrid membrane cryogenic process for post-combustion CO₂ capture. *Procedia Eng.* 44, 417–422. <https://doi.org/10.1016/j.ijproman.2009.11.012>.
- Biermann, M., Normann, F., Johnsson, F., Skagestad, R., 2018. Partial carbon-capture by absorption cycle for reduced specific capture cost. *Ind. Eng. Chem. Res.* 57 (45), 15411–15422. <https://doi.org/10.1021/acs.iecr.8b02074>.
- Cau, G., Tola, V., Ferrara, F., Porcu, A., Pettinau, A., 2018. CO₂-free coal-fired power generation by partial oxy-fuel and post-combustion CO₂ capture: techno-economic analysis. *Fuel* 214, 423–435. <https://doi.org/10.1016/j.fuel.2017.10.023>.
- CEMCAP-SINTEF-ER, 2017. CEMCAP Preliminary Framework for Comparative Techno-Economic Analysis of CO₂ Capture from Cement Plants - Report.
- Doukelis, A., Vorrias, I., Grammelis, P., Kakaras, E., Whitehouse, M., Riley, G., 2009. Partial O₂-fired coal power plant with post-combustion CO₂ capture: A retrofitting option for CO₂ capture ready plants. *Fuel* 88, 2428–2436. <https://doi.org/10.1016/j.fuel.2009.05.017>.
- Dubois, L., 2013. Etude de la capture du CO₂ en postcombustion par absorption dans des solvants aminés : application aux fumées issues de cimenteries. PhD thesis. University of Mons-[FPMS](https://doi.org/10.1017/CBO9781107415324.004)<https://doi.org/10.1017/CBO9781107415324.004>.
- Dubois, L., Thomas, D., 2018. Comparison of various configurations of the absorption-regeneration process using different solvents for the post-combustion CO₂ capture applied to cement plant flue gases. *Int. J. Greenh. Gas Control* 69, 20–35. <https://doi.org/10.1016/j.ijggc.2017.12.004>.
- Dubois, L., Laribi, S., Mouhoubi, S., De Weireld, G., Thomas, D., 2017. Study of the post-combustion CO₂ capture applied to conventional and partial oxyfuel cement plants. *Energy Procedia* 114, 6181–6196. <https://doi.org/10.1016/j.egypro.2017.03.1756>.
- European Commission, 2017. Quarterly report on European electricity markets, market observatory for energy. DG Energy 10, 2.
- Favre, E., Bounaceur, R., Roizard, D., 2009. A hybrid process combining oxygen enriched air combustion and membrane separation for post-combustion carbon dioxide capture. *Sep. Purif. Technol.* 68, 30–36. <https://doi.org/10.1016/j.seppur.2009.04.003>.
- Freeman, S.A., Dugas, R., Van Wagener, D., Nguyen, T., Rochelle, G.T., 2009. Carbon dioxide capture with concentrated, aqueous piperazine. *Energy Procedia* 1, 1489–1496. <https://doi.org/10.1016/j.egypro.2009.01.195>.
- Gardarsdóttir, S.O., De Lena, E., Romano, M., Roussanaly, S., Voldsund, M., Pérez-Calvo, J.-F., Berstad, D., Fu, C., Anantharaman, R., Sutter, D., Gazzani, M., Mazzotti, M., Cinti, G., 2019. Comparison of technologies for CO₂ capture from cement production—part 2: cost analysis. *Energies* 12, 542. <https://doi.org/10.3390/en12030542>.
- Gerbelová, H., van der Spek, M., Schakel, W., 2017. Feasibility assessment of CO₂ capture retrofitted to an existing cement plant: post-combustion vs. Oxy-fuel combustion technology. *Energy Procedia* 114, 6141–6149. <https://doi.org/10.1016/j.egypro.2017.03.1751>.
- Granados, D., Mejía, J., Chejne, F., Gómez, C., Berrío, A., Jurado, W., 2011. Numerical Simulation of Oxy-Fuel Combustion in a Cement Kiln - Conference Paper. pp. 184–187.
- Hassan, S.M.N.H., 2005. Techno-Economic Study of CO₂ Capture Process for Cement Plants. PhD thesis. University of Waterloo, Ontario, Canada.
- Hills, T., Leeson, D., Florin, N., Fennell, P., 2016. Carbon capture in the cement industry: technologies, progress, and retrofitting. *Environ. Sci. Technol.* 50, 368–377. <https://doi.org/10.1021/acs.est.5b03508>.
- Huang, Y., Wang, M., Stephenson, P., Rezvani, S., McIlveen-Wright, D., Minchener, A., Hewitt, N., Dave, A., Fleche, A., 2012. Hybrid coal-fired power plants with CO₂ capture: A technical and economic evaluation based on computational simulations. *Fuel* 101, 244–253. <https://doi.org/10.1016/j.fuel.2010.12.012>.
- Idem, R., Supap, T., Shi, H., Gelowitz, D., Ball, M., Campbell, C., Tontiwachwuthikul, P., 2015. Practical experience in post-combustion CO₂ capture using reactive solvents in large pilot and demonstration plants. *Int. J. Greenh. Gas Control* 40, 6–25. <https://doi.org/10.1016/j.ijggc.2015.06.005>.
- IEAGHG, 2008. CO₂ Capture in the Cement Industry - Technical Study-Report Number 2008/3.
- Karimi, M., Hillestad, M., Svendsen, H.F., 2011. Capital costs and energy considerations of different alternative stripper configurations for post combustion CO₂ capture. *Chem. Eng. Res. Des.* 89, 1229–1236.
- Kemper, J., Ewert, G., Grünwald, M., 2011. Absorption and regeneration performance of novel reactive amine solvents for post-combustion CO₂ capture. *Energy Procedia* 4, 232–239. <https://doi.org/10.1016/j.egypro.2011.01.046>.
- Knudsen, J.N., Jensen, J.N., Vilhelmsen, P.-J., Biede, O., 2009. Experience with CO₂ capture from coal flue gas in pilot-scale: testing of different amine solvents. *Energy Procedia* 1, 783–790. <https://doi.org/10.1016/j.egypro.2009.01.104>.
- Lawal, A., Wang, M., Stephenson, P., Koumpouras, G., Yeung, H., 2010. Dynamic modelling and analysis of post-combustion CO₂ chemical absorption process for coal-fired power plants. *Fuel* 89, 2791–2801. <https://doi.org/10.1016/j.fuel.2010.05.030>.
- Lawal, A., Wang, M., Stephenson, P., 2011. Investigating the dynamic response of CO₂ chemical absorption process in enhanced-O₂ coal power plant with post-combustion CO₂ capture. *Energy Procedia* 4, 1035–1042. <https://doi.org/10.1016/j.egypro.2011.01.152>.
- Li, L., Li, H., Namjoshi, O., Du, Y., Rochelle, G.T., 2013. Absorption rates and CO₂ solubility in new piperazine blends. *Energy Procedia* 37, 370–385. <https://doi.org/10.1016/j.egypro.2013.05.122>.
- Li, K., Leigh, W., Feron, P., Yu, H., Tade, M., 2016. Systematic study of aqueous monoethanolamine (MEA)-based CO₂ capture process: techno-economic assessment of the MEA process and its improvements. *Appl. Energy* 165, 648–659. <https://doi.org/10.1016/j.apenergy.2015.12.109>.
- Mudhasakul, S., Ku, Hming, Douglas, P.L., 2013. A simulation model of a CO₂ absorption process with methyldiethanolamine solvent and piperazine as an activator. *Int. J. Greenh. Gas Control* 15, 134–141. <https://doi.org/10.1016/j.ijggc.2013.01.023>.
- Ortiz, C., Valverde, J.M., Chacartegui, R., Benítez-Guerrero, M., Perejón, A., Romeo, L.M., 2017. The oxy-CaL process: A novel CO₂ capture system by integrating partial oxy-combustion with the calcium-looping process. *Appl. Energy* 196, 1–17. <https://doi.org/10.1016/j.apenergy.2017.03.120>.
- Raynal, L., Bouillon, P.A., Gomez, A., Brouin, P., 2011. From MEA to demixing solvents and future steps, a roadmap for lowering the cost of post-combustion carbon capture. *Chem. Eng. J.* 171, 742–752. <https://doi.org/10.1016/j.ccej.2011.01.008>.
- Smart, J.P.P., Riley, G.S.S., 2012. Use of oxygen enriched air combustion to enhance combined effectiveness of oxyfuel combustion and post-combustion flue gas cleanup part 1 - combustion. *J. Energy Inst.* 85, 123–130. <https://doi.org/10.1179/1743967112Z.000000000026>.
- Song, Y., Chen, C.-C., 2009. Symmetric electrolyte nonrandom two-liquid activity coefficient model. *Ind. Eng. Chem. Res.* 48, 7788–7797. <https://doi.org/10.1021/ie9004578>.
- Sun, L., Doyle, S., Smith, R., 2016. Understanding steam costs for energy conservation projects. *Appl. Energy* 161, 647–655. <https://doi.org/10.1016/j.apenergy.2015.09.046>.
- Van Der Ham, L.V., Romano, M.C., Kvamsdal, H.M., Bonalumi, D., Van Os, P., Goether, E.L.V., 2014. Concentrated aqueous piperazine as CO₂ capture solvent : detailed evaluation of the integration with a power plant. *Energy Procedia* 63, 1218–1222. <https://doi.org/10.1016/j.egypro.2014.11.131>.
- van der Spek, M., 2017. Methodological Improvements to Ex-Ante Techno-Economic Modelling and Uncertainty Analysis of Emerging CO₂ Capture Technologies. PhD Thesis. Utrecht University.
- Vega, F., Rodríguez-Galán, M., Alonso-Fariñas, B., Navarrete, B., Cortés, V., 2013. Oxyfuel Combustion Conference OCC3 Ponferrada (Spain). pp. 9–13.
- Vega, F., Navarrete, B., Alonso-fariñas, B., Rodríguez, M., 2014. Development of partial oxy-combustion technology : design, commissioning and experimental program in a pilot plant. *Energy Procedia* 63, 6344–6348. <https://doi.org/10.1016/j.egypro.2014.11.667>.
- Vega, F., Sanna, A., Maroto-Valer, M.M., Navarrete, B., Abad-Correa, D., 2016. Study of the MEA degradation in a CO₂ capture process based on partial oxy-combustion approach. *Int. J. Greenh. Gas Control* 54, 160–167. <https://doi.org/10.1016/j.ijggc.2016.09.007>.
- Vega, F., Cano, M., Camino, S., Navarrete, B., Camino, J.A., 2018. Evaluation of the absorption performance of amine-based solvents for CO₂ capture based on partial oxy-combustion approach. *Int. J. Greenh. Gas Control* 73, 95–103. <https://doi.org/10.1016/j.ijggc.2018.04.005>.
- Vega, F., Camino, S., Gallego, L.M., Cano, M., Navarrete, B., 2019. Experimental study on partial oxy-combustion technology in a bench-scale CO₂ capture unit. *Chem. Eng. J.* 362, 71–80. <https://doi.org/10.1016/j.ccej.2019.01.025>.
- Voldsund, M., Gardarsdóttir, S.O., De Lena, E., Pérez-Calvo, J.-F., Jamali, A., Berstad, D., Fu, C., Romano, M., Roussanaly, S., Anantharaman, R., Hoppe, H., Sutter, D., Mazzotti, M., Gazzani, M., Cinti, G., Jorda, K., 2019. Comparison of technologies for CO₂ capture from cement production—part 1: technical evaluation. *Energies* 12, 559. <https://doi.org/10.3390/en12030559>.
- Wang, Y., Zhao, L., Otto, A., Robinus, M., Stoltena, D., 2017. A review of post-combustion CO₂ capture technologies from coal-fired power plants. *Energy Procedia* 114, 650. <https://doi.org/10.1016/j.egypro.2017.03.1209>.
- Wilk, A., Więclaw-Solny, L., Tatarczuk, A., Krótki, A., Spietz, T., Chwoła, T., 2017. Solvent selection for CO₂ capture from gases with high carbon dioxide concentration. *Korean J. Chem. Eng.* 34, 2275–2283. <https://doi.org/10.1007/s11814-017-0118-x>.
- Zhang, Y., Chen, H., Chen, C.C., Plaza, J.M., Dugas, R., Rochelle, G.T., 2009. Rate-based process modeling study of CO₂ capture with aqueous monoethanolamine solution. *Ind. Eng. Chem. Res.* 48, 9233–9246. <https://doi.org/10.1021/ie900068k>.
- Zhang, W., Liu, H., Sun, Y., Cakstins, J., Sun, C., Snape, C.E., 2016. Parametric study on the regeneration heat requirement of an amine-based solid adsorbent process for post-combustion carbon capture. *Appl. Energy* 168, 394–405. <https://doi.org/10.1016/j.apenergy.2016.01.049>.